



Providing Choice & Value

Generic CT and MRI Contrast Agents



CONTACT REP

AJNR

**High-Resolution 3D-Constructive
Interference in Steady-State MR Imaging and
3D Time-of-Flight MR Angiography in
Neurovascular Compression: A Comparison
between 3T and 1.5T**

This information is current as
of July 5, 2025.

M. Garcia, R. Naraghi, T. Zumbrunn, J. Rösch, P. Hastreiter
and A. Dörfler

AJNR Am J Neuroradiol published online 8 March 2012
<http://www.ajnr.org/content/early/2012/03/08/ajnr.A2974>

ORIGINAL
RESEARCH

M. Garcia
R. Naraghi
T. Zumbunn
J. Rösch
P. Hastreiter
A. Dörfler



High-Resolution 3D-Constructive Interference in Steady-State MR Imaging and 3D Time-of-Flight MR Angiography in Neurovascular Compression: A Comparison between 3T and 1.5T

BACKGROUND AND PURPOSE: High-resolution MR imaging is useful for diagnosis and preoperative planning in patients with NVC. Because high-field MR imaging promises higher SNR and resolution, the aim of this study was to determine the value of high-resolution 3D-CISS and 3D-TOF MRA at 3T compared with 1.5T in patients with NVC.

MATERIALS AND METHODS: Forty-seven patients with NVC, trigeminal neuralgia, hemifacial spasm, and glossopharyngeal neuralgia were examined at 1.5T and 3T, including high-resolution 3D-CISS and 3D-TOF MRA sequences. Delineation of anatomic structures, overall image quality, severity of artifacts, visibility of NVC, and assessment of the SNR and CNR were compared between field strengths.

RESULTS: SNR and CNR were significantly higher at 3T ($P < .001$). Significantly better anatomic conspicuity, including delineation of CNs, nerve branches, and assessment of small vessels, was obtained at 3T ($P < .02$). Severity of artifacts was significantly lower at 3T ($P < .001$). Consequently, overall image quality was significantly higher at 3T. NVC was significantly better delineated at 3T ($P < .001$). Six patients in whom NVC was not with certainty identifiable at 1.5T were correctly diagnosed at 3T.

CONCLUSIONS: Patients with NVC may benefit from the higher resolution and greater sensitivity of 3T for preoperative assessment of NVC, and 3T may be of particular value when 1.5T is equivocal.

ABBREVIATIONS: CISS = constructive interference in steady state; CN = cranial nerve; CNR = contrast-to-noise ratio; MIP = maximum intensity projection; MVD = microvascular decompression; NVC = neurovascular compression; REZ = root exit zone; SI = signal intensity; TOF = time-of-flight; VRT = volume-rendering technique

Although trigeminal neuralgia, hemifacial spasm, and glossopharyngeal neuralgia can be caused by tumors, vascular malformations, or demyelinating processes, most cases result from NVC.¹ NVC is caused by arteries or veins compressing or indenting nerve roots,^{2,3} usually as they traverse the basal cisterns close to the REZ. A close anatomic relationship or even direct contact between a nerve and a vessel, however, does not necessarily imply that the patient is or will become symptomatic, because this is often seen in asymptomatic patients. Moreover, in some patients with unilateral symptoms, imaging may depict a close neurovascular relationship on both sides. Therefore, the term “NVC” should only be used for symptomatic patients in whom the side of the close neurovascular relationship seen on MR imaging matches the side of the patient symptoms.

Trigeminal neuralgia is the most common of all NVC syndromes and is characterized by paroxysmal facial pain affect-

ing ≥ 1 division of the fifth CN.⁴ Hemifacial spasm^{1,2} and glossopharyngeal neuralgia are less common and result from compression of CN VII and CN IX, respectively, at the REZ.^{2,4-6} Hemifacial spasm manifests as involuntary contractions or paroxysmal spasms of the facial muscles,¹ whereas glossopharyngeal neuralgia is characterized by bursts of lancinating pharyngeal pain.

If medical therapy fails to relieve the pain, then other methods can be offered, including stereotactic radiosurgery and MVD. MVD^{1,4,6} is generally recommended for younger patients with a longer life expectancy and has been shown to be more effective than stereotactic radiosurgery,^{7,8} providing long-term improvement or complete resolution in most cases.^{1,4} Because the presence and severity of NVC highly correlate with the outcome after MVD,⁴ detailed preoperative anatomic evaluation by MR imaging is widely used for precise assessment of neurovascular relationships. Furthermore, accurate delineation of the responsible vessel may decrease the rate of possible operative complications such as nerve paresis.¹

The optimal images for evaluation of neurovascular relationships are high-resolution 3D MRA sequences, which allow visualization of small vessels, and high-resolution heavily T2WI 3D sequences with a very high CSF-tissue contrast such as the CISS sequence or its equivalent, the fast imaging employing steady-state acquisition⁹ sequence which enables the best assessment of an accurate relationship between nerve roots or their branches and adjacent vessels.¹⁰⁻¹²

High-field MR imaging (3T and higher) has the potential

Received September 1, 2011; accepted after revision October 31.

From the Departments of Neuroradiology (M.G., J.R., A.D.) and Neurosurgery (P.H.), Friedrich-Alexander-University of Erlangen-Nuremberg, Erlangen, Germany; Department of General Radiology and Neuroradiology (M.G.), Clinic for Radiology and Nuclear Medicine, and Clinical Trial Unit (T.Z.), University Hospital Basel, Basel, Switzerland; and Department of Neurosurgery (R.N.), Armed Forces Hospital Ulm, Ulm, Germany.

Please address correspondence to Meritxell Garcia, MD, Department of Radiology and Neuroradiology, Clinic for Radiology and Nuclear Medicine, University Hospital Basel, Petersgraben 4, 4031 Basel, Switzerland; e-mail: GarciaMe@uhbs.ch

Indicates article with supplemental on-line tables.

<http://dx.doi.org/10.3174/ajnr.A2974>

to significantly improve clinical care in various neurologic disorders^{13,14} because it offers increased diagnostic sensitivity and specificity due to its higher SNR,^{15,16} and improvements at 3T have already been established for several MRA sequences^{15,17} and 3D-T2WI.^{6,18}

The aim of this study was to determine the diagnostic performance of high-resolution 3D-CISS and 3D-TOF MRA at 3T compared with 1.5T MR imaging in NVC, both quantitatively and qualitatively.

Materials and Methods

Subjects and Imaging Protocol

The study was approved by our institutional review board, and informed consent was obtained from all patients after the investigative character of the study had been fully explained. Forty-seven symptomatic patients (24 women, 23 men; mean age, 55.2 years) with NVC (36 with trigeminal neuralgia, 8 with hemifacial spasm, 3 with glossopharyngeal neuralgia) were prospectively examined on both 1.5T and 3T scanners (Sonata and Magnetom Tim Trio; Siemens, Erlangen, Germany). To exclude other pathologies causing nerve compression, conventional T1WI with and without contrast enhancement and T2WI were additionally performed at the first MR imaging examination (1.5T or 3T only). The time interval between the 2 examinations was <36 hours in 31 patients, between 1 and 3 weeks in 8 patients, between 3 and 4 months in 3 patients, between 8 and 15 months in 3 patients, 2.5 years in 1 patient, and 3.5 years in 1 patient.

Imaging parameters were kept as similar as possible at approximately similar acquisition times.¹⁹ The detailed MR image parameters for the 3D-CISS and 3D-TOF MRA are given in Tables 1 and 2.

Image Analysis

Qualitative Assessment. The score for the overall image quality, based on the conspicuity of anatomic structures and the severity of pulsation and motion artifacts, was assessed in all 47 patients. A separate score representing the presence and severity of artifacts only was additionally assessed in all 47 patients. For anatomic assessment, the following structures were evaluated on both the 3D-CISS and 3D-TOF MRA: posterior cerebral artery, superior cerebellar artery, anterior inferior cerebellar artery, posterior inferior cerebellar artery, cavernous sinus, and the boundary between the cavernous sinus and the ICA. For the 3D-CISS images, we additionally assessed the following anatomic structures: CN V, branches of CN V (V1, V2, V3), CN VII, CN IX, CN X, as well as identification and conspicuity of the NVC. When a nerve compression by a vessel was clearly delineated in the 3D-CISS, then the relevant vessel was scrutinized on the 3D-TOF MRA for determination of its origin and verification of the suspected diagnosis of NVC.

Overall image quality, severity of artifacts, anatomic structures, and visibility of NVC were each graded on a 4-point scale according to the following: 1 = nondiagnostic/not distinguishable/image quality severely impaired, 2 = questionable for diagnosis/questionably visible/many artifacts, 3 = adequate for diagnosis/adequately visible/minor artifacts, and 4 = excellent/no artifacts. Each set of images was assessed for all items by an experienced neuroradiologist, who was only provided with the presumed diagnosis and affected side (right or left) and blinded to all other clinical findings. The NVC was only assessed on the symptomatic side. If close contact between a CN and a vessel was also observed in the contralateral asymptomatic side, this side was not evaluated for NVC.

Table 1: Sequence parameters for the 3D-CISS at 1.5T and 3T

Parameters	1.5T	3T
Acquisition time (min:sec)	7:03	8:26
Voxel size (mm ³)	0.4	0.4
No. of slabs	1	1
Sections per slab	144	144
Distance factor (%)	20	20
FOV read (mm)	230	200
FOV phase (%)	62.5	100
Section thickness (mm)	0.4	0.4
Base resolution	512	512
Phase resolution (%)	100	100
Section resolution (%)	64	50
TR (ms)	9.65	7.48
TE (ms)	4.83	3.23
No. of averages	1	1
Flip angle (°)	90	45
Bandwidth (Hz/px)	163	250
No. of averages	1	1
No. of measurements	1	1
SNR	1	1
Phase oversampling (mm ³)	0	0
Section oversampling (%)	0	22.2
Phase partial Fourier	7/8	7/8
Section partial Fourier	7/8	7/8

In a separate session, overall image quality, severity of artifacts, and visibility of the NVC of the 31 patients in whom the 2 examinations were performed within 36 hours of each other were additionally evaluated immediately after the examination and in consensus by the above-mentioned neuroradiologist and the neurosurgeon, who performed the MVD in the patients who underwent surgery. The neurosurgeon was aware of all available patient data.

Quantitative Analysis. Quantitative assessment of the SNR of the basilar artery, the CNR between the basilar artery and brain stem, and the CNR between the CSF and ICA was performed by calculation, whereby the SNR was defined as the SI of the respective structure

Table 2: Sequence parameters for the 3D-TOF MRA at 1.5T and 3T

Parameters	1.5T	3T
Acquisition time (min:sec)	15:07	15:51
Voxel size (mm ³)	0.4	0.4
No. of slabs	1	1
Sections per slab	144	144
Distance factor (%)	50	50
FOV read (mm)	230	200
FOV phase (%)	62.5	100
Section thickness (mm)	0.4	0.4
Base resolution	512	512
Phase resolution (%)	100	100
Section resolution (%)	67	50
TR (ms)	40	21
TE (ms)	7.15	3.77
Flip angle (°)	25	18
Bandwidth (Hz/px)	65	212
MTC	Yes	No
No. of averages	1	1
No. of concatenations	1	1
No. of measurements	1	1
SNR	1	1
Phase oversampling (mm ³)	0	0
Section oversampling (%)	0	22.2
Phase partial Fourier	7/8	Off
Section partial Fourier	7/8	Off

Note:—MTC indicates magnetization transfer contrast.

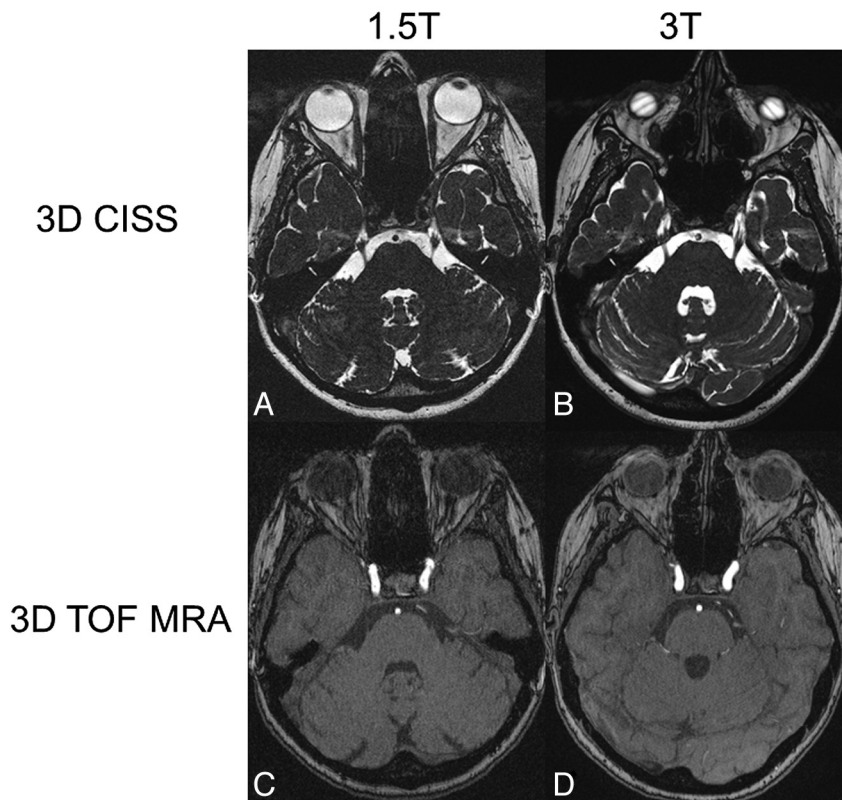


Fig 1. Axial source images of 3D-CISS sequences at the level of the trigeminal nerve root (A and B) and 3D-TOF MRAs at the level of the cavernous sinus (C and D) at 1.5T (A and C) and 3T (B and D) in the same patient. Note the ramification of the nerve root into its branches at some distance from the REZ. The branches are much better outlined at 3T than at 1.5T in the 3D-CISS sequence (A and B). The vessels and the boundary between the cavernous sinus and ICA can be distinguished more accurately at 3T than at 1.5T in the 3D-TOF MRA (C and D). Note the banding artifacts over the globes in the 3D-CISS at 3T (B). Ghosting artifacts are seen anterior to the CSF in the 3D-CISS at both field strengths (A and B).

divided by the SD of background noise ($SNR = SI/SD$), and the CNR, by the difference in the SI between 2 selected structures divided by the SD of background noise ($CNR = \frac{SI_{structure 1} - SI_{structure 2}}{SD}$). The regions of interest were of the same size and in the same location at both field strengths in all patients.

Statistics

Comparison between 1.5T and 3T for each sequence was conducted for each variable by means of the paired Wilcoxon signed rank tests (with continuity correction). The *P* values for all tests were adjusted with the method of Benjamini and Yekutieli,²⁰ by controlling the overall false discovery rate. Application of parametric tests for the continuous variables (SNR, CNR) was not considered because their distribution was highly skewed. Differences were considered significant when the *P* value was $<.05$.

Results

The results of the Wilcoxon signed rank test for all comparisons are summarized in On-line Table 1 for the 3D-CISS and in On-line Table 2 for the 3D-TOF MRA.

Overall Image Quality and Severity of Artifacts

Overall image quality, consisting of the degree of clarity of fine anatomic details and the presence of various artifacts, was significantly ($P < .001$) higher at 3T than at 1.5T for both sequences. When evaluating the exclusive presence and severity of artifacts, we found that significantly more and also more severe artifacts were apparent at 1.5T for both sequences. This

finding partially contributed to the significantly poorer overall image quality at 1.5T ($P < .001$).

Assessment of Fine Anatomic Details

Cavernous Sinus and the Boundary between the Cavernous Sinus and ICA. The anatomy of the cavernous sinus ($P = .003$ for the TOF and $P < .001$ for the CISS sequence) and the conspicuity of the boundary between the cavernous sinus and ICA ($P = .001$ for both sequences) (Fig 1C, -D) were significantly better delineated at 3T than at 1.5T, due to the sharper contrast and fewer artifacts at 3T.

Arteries in the Posterior Fossa and Brain Stem Area. The arteries in the posterior fossa and around the brain stem (posterior cerebral artery, superior cerebellar artery, anterior inferior cerebellar artery, and posterior inferior cerebellar artery) were significantly better scored at 3T than at 1.5T for the CISS sequence ($P < .008$) and the TOF-MRA ($P < .001$) sequence, mainly due to the markedly higher contrast between tissues (Fig 2). In the 3D-TOF MRA, more vessels were visible at 3T compared with 1.5T (Fig 2C, -D). In some patients, small-caliber branches of larger vessels that were hardly or not visible at all at 1.5T could be clearly identified and characterized (artery or vein) at 3T.

Cranial Nerves. The CNs assessed in the 3D-CISS sequence (CN V and its branches [V1, V2, V3], CN VII, CN IX, and CN X) yielded significantly higher scores at 3T than at 1.5T ($P < .02$) due to the superior definition of the CN itself and sharper boundaries between the CNs and their surround-

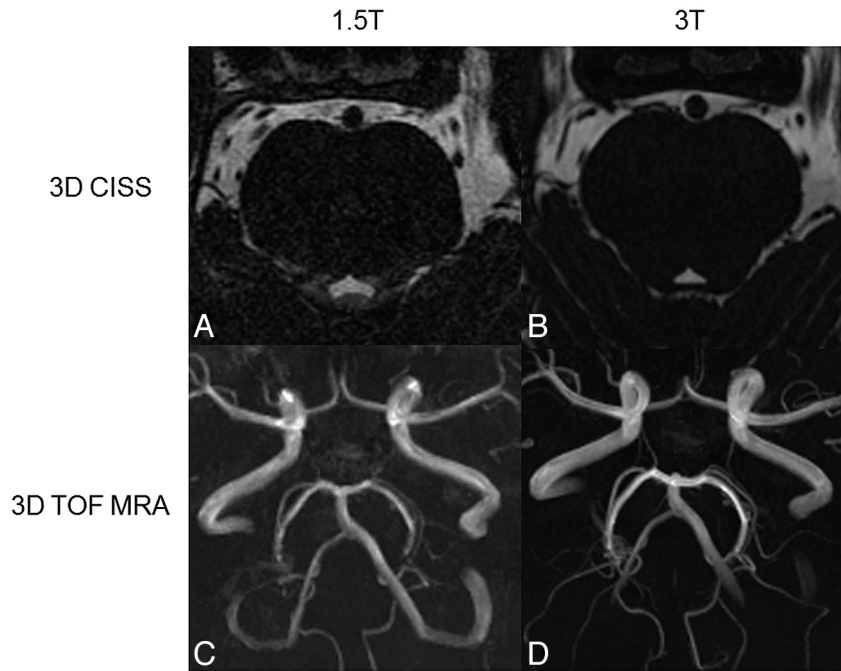


Fig 2. Axial source images of 3D-CISS sequences (A and B) and MIP of 3D-TOF MRAs (C and D) obtained at 1.5T (A and C) and 3T (B and D). The contours of the anatomic structures can be more accurately delineated at 3T compared with 1.5T. Note that more vessels can be delineated in the MIP obtained at 3T (D) compared with 1.5T (B).

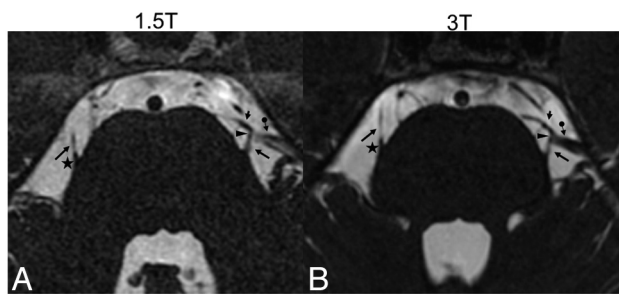


Fig 3. Axial source images of the 3D-CISS sequence at 1.5T (A) and 3T (B) of a patient with trigeminal neuralgia on the left side showing a close relationship (arrowhead) between the upper part of the trigeminal nerve (trigeminal neuralgia, long arrow) and a larger vein (arrow with dot) and a smaller artery (short arrow) on the left side at some distance from the REZ (asterisk, shown on the contralateral side). The proximate adjacency between the trigeminal neuralgia and the small artery is visible at both field strengths. However, the direct contact between the trigeminal neuralgia and vein is questionable at 1.5T (arrowhead in A), whereas the direct nerve-vein contact is clearly visible at 3T (arrowhead in B), confirming the diagnosis of NVC.

ings, mainly CSF. Similarly, the single branches of CN V could be significantly better differentiated from the surrounding CSF at 3T (Fig 1A, -B).

Assessment of the NVC. The NVC in the 3D-CISS sequence was significantly ($P < .001$) better defined at 3T compared with 1.5T (Fig 3). There were no patients in whom a close neurovascular relationship was excluded at 1.5T but clearly visible at 3T. In 6 of the 47 patients (12.8%) in whom the neurovascular relationships were not sufficiently defined to make a certain diagnosis of NVC at 1.5T, the NVC could be diagnosed with certainty at 3T. These 6 patients presented with trigeminal neuralgia, and the 3D-CISS images at 3T clearly showed a direct contact between CN V and a vein or a branch of the superior cerebellar artery not directly at the REZ but a few millimeters away from the REZ (Fig 3). In these 6 cases, the time interval between the 2 examinations was

<36 hours. In all cases (in 47 patients at 3T and in 41 patients at 1.5T) in which a direct nerve compression by a vessel was clearly detected in the 3D-CISS images at 1.5T and 3T (Fig 4), respectively, the origin of the vessel could be reliably determined in the 3D-TOF MRA.

Assessment of Absolute Values: SNR and CNR. Compared with 1.5T, at 3T the SI of the basilar artery was markedly higher in the 3D-CISS sequence and, in most cases, higher in the 3D-TOF MRA. Overall, the SD of background noise was lower and differences in SI between evaluated structures (CSF versus ICA, basilar artery versus brain stem) were higher at 3T compared with 1.5T (data not shown). Consequently, the SNR of the basilar artery and the CNR between the CSF and ICA were >5 times higher, and the CNR between the basilar artery and brain stem >6 times higher in the 3D-CISS at 3T than at 1.5T. For the 3D-TOF MRA, the calculated SNR and CNR were also significantly ($P < .001$) higher at 3T; however, the differences were less pronounced (Fig 5).

Discussion

In this study the diagnostic value of high-resolution 3D-CISS and 3D-TOF MRA at 3T compared with 1.5T in NVC is assessed. Some patients with trigeminal neuralgia, hemifacial spasm, and glossopharyngeal neuralgia have lesions visible on conventional MR imaging, but in most cases, the symptoms are caused by NVC and this condition usually requires further evaluation with high-resolution MR imaging. Although NVC is often caused by larger arteries, it may be also caused by smaller arterial branches or veins. High-resolution 3D-MRA (eg, 3D-TOF MRA) and 3D-T2WI (eg, 3D-CISS) are well-established sequences used for the preoperative assessment of NVC.^{14,15,21-23} The sections can be very thin (<1 mm) and without gaps, thereby ensuring high resolution. Because some of the compressing vessels have a diameter <2 mm, a section

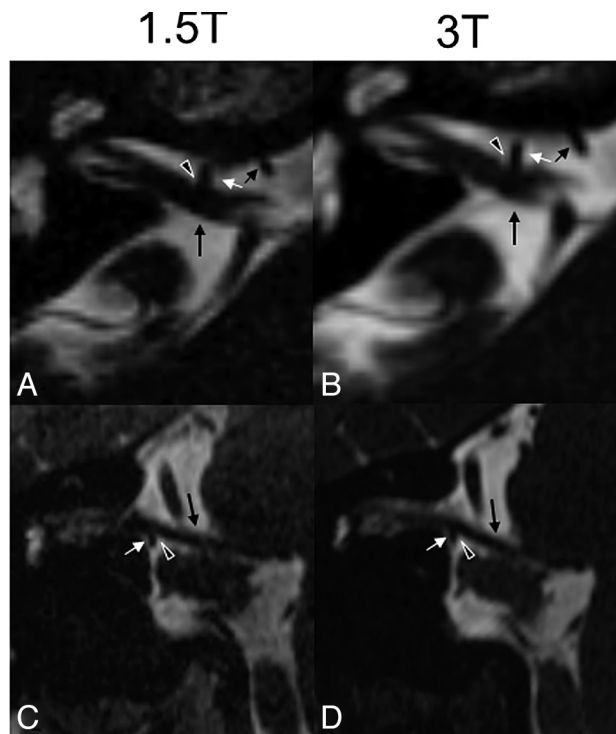


Fig 4. Axial source (A and B) and coronal (C and D) reformatted CISS images at 1.5T (A and C) and 3T (B and D) of a patient with hemifacial spasm on the right side due to a direct contact (black arrowhead with white margins) between the VII-VIII nerve complex (long black arrow) and the meatal segment of the anterior inferior cerebellar artery (short white arrow), forming a loop near the nerve complex (short black and white arrows in A and B, in which the short black arrow indicates the proximal part and the short white arrow, the distal part of the anterior inferior cerebellar artery). In this patient, the NVC is approximately equally well seen at both field strengths.

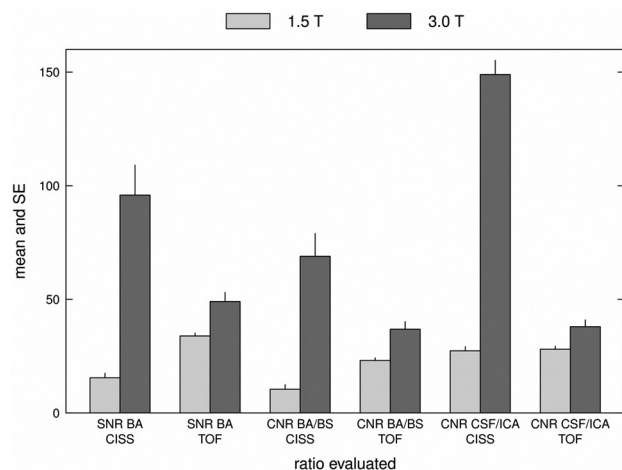


Fig 5. Bar graph showing the mean (\pm standard error) of the SNR of the basilar artery, CNR between the basilar artery and brain stem, and CNR between the CSF and ICA for both the 3D-CISS and 3D-TOF MRA. Note the higher SNR and CNR for all items at 3T, though they are more pronounced for the 3D-CISS than for the 3D-TOF MRA.

thickness of 3 mm in conventional MR imaging may miss the pathology.⁶

The most important advantage of high-field MR imaging is its high SNR,^{16,24-26} which can be used to scan at higher resolution and/or increased speed. Given the different properties between field strengths, imaging parameters and examination times were kept as equal as possible to most accurately assess the extent of potential advantage of 3T over 1.5T in NVC.

3D-CISS is a heavily T2WI sequence with very high resolution and CSF-tissue contrast, providing detailed visualization especially of structures surrounded by CSF.^{4,6,19,21}

There are few studies of the beneficial properties of 3D-CISS at 3T in patients with NVC,^{3,4,27} and to date, no data about the possible improvement of 3D-CISS at 3T over 1.5T in the same patient population with NVC are available. The increased SNR at higher field strengths is useful for the conspicuity of small anatomic structures.¹⁶ In this study, all assessed vessels and CNs could be better delineated at 3T. In 6 cases of trigeminal neuralgia, NVC was not sufficiently well-defined at 1.5T due to partial blurring of the anatomic details; in these patients, the diagnosis of NVC was questionable or equivocal at 1.5T but could be defined at 3T. In these patients, the NVC was not caused by a typical nerve-vessel contact at the REZ but rather by a vein or minuscule arterial branch at some distance from the REZ that could be reliably delineated at 3T. All patients underwent MVD, and the neurovascular relationship assessed in the 3D-CISS at 3T coincided with the surgical observation, a finding supporting the diagnostic advantage of 3T.

A drawback of 3D-CISS are banding artifacts, which are more pronounced at high-field MR imaging due to increased susceptibility. Dark bands were seen in some patients at 3T over the ocular globe (Fig 1B), which were easily detectable and did not interfere with diagnostic quality. No banding artifacts were seen in the basal cisterns. Aliasing artifacts at 3T could be eliminated by lowering the flip angle (Table 1). Ghosting artifacts resulting from CSF pulsation were seen at both 1.5T and 3T anterior to the CSF in the phase-encoding direction (Fig 1A, -B). Although these artifacts were sometimes slightly wider at 3T, they could be much better separated from the underlying brain tissue, and this, together with the higher SNR and CNR, still resulted in better image quality at 3T.

Due to the more homogeneous hypointensity of the lumina of the basilar artery and the vertebral arteries at 1.5T, the center of these vessels was better seen at 1.5T. In contrast, at 3T a high signal intensity within the basilar artery and vertebral arteries was seen in almost all patients for the length of a few sections only, most likely due to flow pulsation and absent dephasing effects. Because this high SI was located in the center of the lumen only, the strong vessel-CSF contrast was still preserved, and this did not compromise detection of NVC.

For 3D-TOF MRA, the signal-intensity gain at 3T has been shown to provide a significantly improved vessel-tissue contrast compared with 1.5T.^{16,17,24,25,28,29} There are limited data concerning the value of 3D-TOF MRA at 3T in NVC,^{3,4,27} and, to our knowledge, no comparison between 1.5T and 3T in the same patient population with NVC has been conducted to date. In our study, anatomic structures were significantly ($P < .02$) better visible and quantitative values were significantly ($P < .001$) higher at 3T, resulting in a substantially improved image quality. The 3T MRA provided a better separation between veins and small arteries, and small vascular branches hardly or not visible at 1.5T could be delineated at 3T (Fig 2C, -D). When NVC was clearly depicted in the 3D-CISS, rapid verification of the responsible vessel was possible at 3T, whereas this was far less straightforward at 1.5T.

The superior image quality for the 3D-TOF MRA at 3T is largely due to the decreased longitudinal relaxation with in-

creased field strength, producing longer T1 times. The short TRs at 3T (Table 2) saturate the stationary tissue but not the circulating blood to a greater extent than at 1.5T, thereby enhancing vessel-tissue contrast. Although flow artifacts in the 3D-TOF MRA may be more pronounced at 3T due to increased susceptibility and SNR,²⁸ in this study no substantial or more severe artifacts at 3T compared with 1.5T were observed.

A drawback of our study is the long scanning time. Due to technical improvements, however, both sequences can be obtained with an acquisition time of <10 minutes at present. In 5 patients, there was a time interval of >6 months between the 2 studies; because these patients were already diagnosed with NVC at 1.5T and because they denied any progression of their symptoms, they were not excluded from the study. We did not classify NVCs according to their distance from the REZ, but our aim was to focus on imaging features and not on clinical-surgical correlations.

Implications for Patient Care

3T proved to be superior to 1.5T for the assessment of NVC. The higher resolution at 3T provided an improvement in image quality compared with 1.5T at similar acquisition times. In 6 patients in whom the NVC could not be identified with certainty at 1.5T due to partial blurring of the contours of the fine anatomic details, the NVC could be verified at 3T. Thus, 3T MR imaging may remove uncertainties and increase diagnostic accuracy. The better image quality and sensitivity at 3T may improve preoperative evaluation of neurovascular relationships. Thus, whenever possible, preoperative evaluation of NVC should be performed at 3T to increase the diagnostic accuracy and ensure the best postoperative outcome.

Conclusions

High-resolution 3D-CISS and 3D-TOF MRA are necessary tools for the assessment of neurovascular relationships in NVC. Patients with NVC may benefit from the higher resolution and greater sensitivity of 3T, especially in those circumstances in which findings are equivocal at 1.5T. Due to the increasing availability of high-field scanners, patients with suspected NVC should be evaluated at 3T when possible to support accurate diagnosis, careful preoperative planning, and best patient care.

Disclosures: Thomas Zurnbrunn—RELATED: Grant: Swiss National Science Foundation.

References

1. Tarnaris A, Renowden S, Coakham HB. A comparison of magnetic resonance angiography and constructive interference in steady state-three-dimensional Fourier transformation magnetic resonance imaging in patients with hemifacial spasm. *Br J Neurosurg* 2007;21:375–81
2. Naraghi R, Tanrikulu L, Troesch-Weber R, et al. Classification of neurovascular compression in typical hemifacial spasm: three-dimensional visualization of the facial and the vestibulocochlear nerves. *J Neurosurg* 2007;107:1154–63
3. Kakizawa Y, Seguchi T, Kodama K, et al. Anatomical study of the trigeminal and facial cranial nerves with the aid of 3.0-Tesla magnetic resonance imaging. *J Neurosurg* 2008;108:483–90
4. Miller J, Acar F, Hamilton B, et al. Preoperative visualization of neurovascular anatomy in trigeminal neuralgia. *J Neurosurg* 2008;108:477–82
5. Satoh T, Onoda K, Date I. Fusion imaging of three-dimensional magnetic resonance cisternograms and angiograms for the assessment of microvascular decompression in patients with hemifacial spasms. *J Neurosurg* 2007;106:82–89
6. Yamakami I, Kobayashi E, Hirai S, et al. Preoperative assessment of trigeminal neuralgia and hemifacial spasm using constructive interference in steady state-three-dimensional Fourier transformation magnetic resonance imaging. *Neurol Med Chir* 2000;40:554–55
7. Pagni CA, Fariselli L, Zeme S. Trigeminal neuralgia: non-invasive techniques versus microvascular decompression—it is really available any further improvement? *Acta Neurochir Suppl* 2008;101:27–33
8. Liu JK, Apfelbaum RI. Treatment of trigeminal neuralgia. *Neurosurg Clin N Am* 2004;15:319–34
9. Benes L, Shiratori K, Gurschi M, et al. Is preoperative high-resolution magnetic resonance imaging accurate in predicting neurovascular compression in patients with trigeminal neuralgia? A single-blind study. *Neurosurg Rev* 2005;28:131–36
10. Anderson VC, Berryhill PC, Sandquist MA, et al. High-resolution three-dimensional magnetic resonance angiography and three-dimensional spoiled gradient-recalled imaging in the evaluation of neurovascular compression in patients with trigeminal neuralgia: a double-blind pilot study. *Neurosurgery* 2006;58:666–73
11. Hastreiter P, Naraghi R, Tomandl B, et al. Analysis and 3-dimensional visualization of neurovascular compression syndromes. *Acad Radiol* 2003;10:1369–79
12. Naraghi R, Hastreiter P, Tomandl B, et al. Three-dimensional visualization of neurovascular relationships in the posterior fossa: technique and clinical application. *J Neurosurg* 2004;100:1025–35
13. Stankiewicz JM, Glanz BI, Healy BC, et al. Brain MRI lesion load at 1.5T and 3T versus clinical status in multiple sclerosis. *J Neuroimaging* 2011;21:e50–56
14. Stobo DB, Lindsay RS, Connell J, et al. Initial experience of 3 Tesla versus conventional field strength magnetic resonance imaging of small functioning pituitary tumours. *Clin Endocrinol (Oxf)* 2011;75:673–77
15. Ross JS. The high-field-strength curmudgeon. *AJNR Am J Neuroradiol* 2004;25:168–69
16. Frayne R, Goodyear BG, Dickhoff P, et al. Magnetic resonance imaging at 3.0 Tesla: challenges and advantages in clinical neurological imaging. *Invest Radiol* 2003;38:385–401
17. Willinek WA, Gieseke J, von Falkenhausen M, et al. Sensitivity encoding (SENSE) for high spatial resolution time-of-flight MR angiography of the intracranial arteries at 3.0 T. *Rofo* 2004;176:21–26
18. Pattany PM. 3T MR imaging: the pros and cons. *AJNR Am J Neuroradiol* 2004;25:1455–56
19. Schwindt W, Kugel H, Bachmann R, et al. Magnetic resonance imaging protocols for examination of the neurocranium at 3 T. *Eur Radiol* 2003;13:2170–79
20. Benjamini Y, Yekutieli D. The control of the false discovery rate in multiple testing under dependency. *Ann Stat* 2001;29:1165–88
21. Leal PR, Hermier M, Froment JC, et al. Preoperative demonstration of the neurovascular compression characteristics with special emphasis on the degree of compression, using high-resolution magnetic resonance imaging: a prospective study, with comparison to surgical findings, in 100 consecutive patients who underwent microvascular decompression for trigeminal neuralgia. *Acta Neurochir (Wien)* 2010;152:817–25. Epub 2010 Jan 28
22. Tanrikulu L, Hastreiter P, Richer G, et al. Virtual neuroendoscopy: MRI-based three-dimensional visualization of the cranial nerves in the posterior cranial fossa. *Br J Neurosurg* 2008;22:207–12
23. Hastreiter P, Naraghi R, Tomandl B, et al. 3D-visualization and registration for neurovascular compression syndrome analysis. In: *MICCAI '02 Proceedings of the 5th International Conference on Medical Image Computing and Computer-Assisted Intervention-Part I*. London, UK: Springer-Verlag; 2002;5:396–403
24. Willinek WA, Schild HH. Clinical advantages of 3.0 T MRI over 1.5 T. *Eur J Radiol* 2008;65:2–14
25. Schmitz BL, Aschoff AJ, Hoffmann MH, et al. Advantages and pitfalls in 3T MR brain imaging: a pictorial review. *AJNR Am J Neuroradiol* 2005;26:2229–37
26. Tanenbaum LN. Clinical 3T MR imaging: mastering the challenges. *Magn Reson Imaging Clin N Am* 2006;14:1–15
27. Leal PR, Hermier M, Souza MA, et al. Visualization of vascular compression of the trigeminal nerve with high-resolution 3T MRI: a prospective study comparing preoperative imaging analysis to surgical findings in 40 consecutive patients who underwent microvascular decompression for trigeminal neuralgia. *Neurosurgery* 2011;69:15–26
28. Willinek WA, Born M, Simon B, et al. Time-of-flight MR angiography: comparison of 3.0-T imaging and 1.5-T imaging—initial experience. *Radiology* 2003;229:913–20
29. Al-Kwif O, Emery DJ, Wilman AH. Vessel contrast at three Tesla in time-of-flight magnetic resonance angiography of the intracranial and carotid arteries. *Magn Reson Imaging* 2002;20:181–87